

J. Telegdi
T. Rigó
É. Pfeifer
T. Keszthelyi
E. Kálmán

Nanolayer Coatings

Abstract Langmuir–Blodgett and self assembled molecular layers of hydroxamic and phosphonic acids deposited onto metal surfaces were studied in corrosive aqueous solution with and without corrosion relevant microorganisms. The role of intermolecular interaction, molecular layer thickness, self assembled molecular layer (SAM) formation time as well as the alkyl chain length in the anticorrosion processes and in the microbiological adhesion was in the focus of our experiments. Langmuir films characterized by isotherms and Brewster angle microscopy (BAM) were deposited as Langmuir–Blodgett (LB) layers onto copper and iron surfaces. The SAM layer formation was followed by sum frequency vibration (SFG) and infrared (IRRAS) spectroscopy, the morphology of the LB and SAM films was visualized by atomic force microscopy (AFM), and the change

in the wettability was characterized by contact angle values measured in pure water on metals (with and without nanocoatings). The anticorrosion efficiency of the nanofilms was confirmed by electrochemical as well as by AFM measurements. The decrease in the microbial adhesion caused by the nanolayers was visualized by epifluorescence microscopy and enumerated by microbiological technique. Correlation was found between the metal surface energy and the number of adhered corrosion relevant microorganisms.

Keywords Anticorrosion efficacy · Hydroxamic and phosphonic acids · Inhibition of microbial adhesion · Intermolecular interaction · Langmuir · Langmuir–Blodgett · SAM layers

J. Telegdi (✉) · T. Rigó · É. Pfeifer · T. Keszthelyi · E. Kálmán
Institute of Surface Chemistry and Catalysis, Department of Surface Modification and Nanostructures, Chemical Research Center, Hungarian Academy of Sciences, P.O. Box 17, 1525 Budapest, Hungary
e-mail: telegdi@chemres.hu

Introduction

The importance of nanolayers in different technologies (coatings, sensors etc.) has increased in the last decades. Mainly two types of nanofilm are discussed in the literature, the Langmuir–Blodgett and the self assembled layers. The early literature on Langmuir monomolecular layers on LB films was reviewed by Gaines [1] and Petty [2]. Roberts also contributed to the LB film topic [3]. Ulman who has discussed both the LB and SAM layers has given an introduction to many characterization techniques [4],

and Schwartz has presented a review on LB film structures [5]. The preparation, characterization and application of LB films have been surveyed by several authors [6–9]. All these papers discuss not only the molecules which can form nanofilms but also the techniques applicable for investigation of molecular layers. Over the last two decades the sensitivity of a number of experimental techniques has been increased. These techniques include photoelectron spectroscopy, X-ray diffraction and reflection, neutron reflection, infra red and Raman spectroscopy, electron diffraction and different scanning probe microscopy. By

fluorescence and Brewster angle microscopy larger structures of nanolayers can be observed, and in special cases the quartz crystal nanobalance can also provide important information on film formation. All these methods help in understanding the LB and SAM layer formation and, on one hand, in elucidating the binding forces between solids and nanolayers, and, on the other hand, in showing the conformation of the amphiphiles in nanolayers.

In our experiments two types of amphiphilic molecules were used for nanolayer preparation. Phosphonic acids have often been discussed in the literature [10–16]. First Lossen reported the existence of hydroxamic acids (acyl hydroxylamines) in 1868 [17]. Biological activities of natural hydroxamic acids were also demonstrated by several authors [18–21]. Extended research on water soluble mono- and dihydroxamic acids were done by Farkas and her co-workers [22–25]. The corrosion inhibiting efficiency of benzohydroxamic acid derivatives and dihydroxamic acids in aqueous solution were also studied [26, 27], but on nanolayers of hydroxamic acids only limited publications are available. The first experiments on hydroxamic acid SAM nanolayers were reported by Folkers et al. [28] who have demonstrated that the SAM layers of alkyl hydroxamic acids are more stable on metal oxide surfaces than the similar carboxylic and phosphonic acids. The most recent publication on alkyl hydroxamic acids [29] discusses monomer and polymer hydroxamic acid in SAMs.

In our previous publications we have shown how can the pH and the subphase temperature influence the molecular layer structure [30] and in some cases the application of these nanolayers was also demonstrated [31, 32]. In this paper intermolecular constants calculated for L monolayers of hydroxamic acid amphiphiles as well as comparative analysis of anticorrosion efficiency of LB and SAM films produced from the same amphiphiles will be presented. Additionally, the influence of the solid surface energy of metals (with and without nanocoatings) on the microbial adhesion will be discussed.

Experimental

Chemicals: alkyl hydroxamic acids (decanoyl (C10N), lauroyl (C12N), palmitoyl (C16N) and stearoyl (C18N) hydroxamic acids) synthesized from the proper alkyl acid chloride and hydroxyl amine [33] were re-crystallized from ethyl acetate. Octadecanoyl phosphonic acid (C18P) was the product of a Michaelis–Arbusov reaction. Melting points, thin layer chromatography, elemental analysis and IR spectroscopy were applied for purity control.

Metal surface finishing: copper (99.99%) and iron (99.99%) surfaces ground with emery paper (200–1200 grit SiC) and polished with Al₂O₃ paste (0.3 μm), were washed with water, degreased with acetone and let it dry under atmospheric conditions.

Nanolayer Preparation

Langmuir and Langmuir–Blodgett Molecular Films

Nanolayers at the air/water interface prepared by spreading a solution of the amphiphiles (dissolved in chloroform) on an ultra pure aqueous subphase were investigated in LB trough (NIMA Technology 611D) equipped with Wilhelmy plate pressure sensor. After spreading and evaporation of the solvent (10 min) the monolayer was compressed and transferred to the polished solid metal surfaces under accurate automatic control of surface pressure which is essential for proper LB deposition, as during film transfer the area of the monolayer is reduced continuously in order to keep the surface pressure at a constant value. To produce high quality LB films the deposition speed is also an essential factor (20 mm/min). The morphology of the Langmuir monomolecular layers were characterized by Brewster angle microscopy (BAM, miniBAM, Göttingen). This technique is a well established method to visualize nanolayers with different structures (condensed domains, scattered molecules etc.). The principle of the operation of BAM is that p-polarized light at the Brewster angle is not reflected from the interface. The water surface is very smooth and has an optically well-defined background signal at the Brewster angle. The areas of different brightness are due to different molecular layer densities on the surface. A single molecular layer is resolved in high contrast. This is an ideal instrument for on-line visualization of homogeneity and of domain structure in nanolayers. In our experiments at different pH and temperature values of the subphase in situ BAM images were taken at the gas-, liquid- and solid phases as well as after the collapse of the molecular layers.

SAM Layer Preparation

Polished, washed and degreased copper and iron coupons were dipped into the solution of amphiphilic materials dissolved in tetrahydrofuran (Merck). The completeness of a compact layer formation was followed by infra red (Nicolet Magna 750 FTIR spectrometer equipped with a liquid nitrogen cooled MCT detector) and sum frequency vibration spectroscopy (EKS-PLA, Vilnius Lithuania). The maximum intensity of peaks in SFG spectra has proven the compactness of the nanolayers.

The solid surface morphology (with and without nanocoatings) were visualized by atomic force microscopy (AFM, Digital Instruments, NanoScope III).

Electrochemical Experiments

In a three-necked cell filled with 300 ml sodium sulphate electrolyte (0.1 M; pH = 3.5 (copper); pH = 7.0 (iron); room temperature) were immersed the working electrode

(copper or iron with and without nanolayers), the counter electrode (Pt) and the reference (saturated calomel) electrode. The corrosion potential and the polarisation curves were registered in a potentiostat (Radiometer PG-201). Polarization resistance values were calculated from electrochemical impedance spectra (EIS).

Microbial Adhesion Experiments

Metal coupons with or without nanolayers were immersed either into cooling water (with mixed population of corrosion relevant microorganisms) or into pure culture of *Desulfovibrio desulfuricans*, *Acidithiobacillus ferrooxidans* and *Leptospirillum ferrooxidans*. The presence of adhered microbes was demonstrated by epifluorescence microscope (Zeiss) after acridine orange staining (0.01% acridine orange in water).

Results and Discussion

Several experimental techniques have enabled us to obtain detailed information on Langmuir and Langmuir–Blodgett films. The influence of pH and temperature of the subphase is important to know in order to find the most proper conditions for the preparation of the most compact Langmuir and LB layers.

Isotherms Measured at Different pH and Temperature

After spreading long-chain hydroxamic acids on pure water sub-phase, the Langmuir monolayers were characterized by surface pressure/area (Π/A) isotherm at different

temperatures (Fig. 1). The slope of the isotherms is temperature dependent, different phase transitions can be observed if the temperature varies, similarly to results given in the literature for other molecules [34, 35].

On pure water surface the pressure/area isotherms show three distinct regions, which can be described as gas-, liquid- and solid-phase. The transition pressure between liquid and solid phase is 20 mN/m in the case of the C16 N, and 18 mN/m at C18 N. For the sake of comparison similar value of the stearic acid is 23 mN/m [36]. This transition is temperature-dependent, and the molecules need larger surface area at higher temperature. The decrease in the temperature results in a more rigid Langmuir monolayer. The collapse pressure of the monolayers on pure water sub-phase at pH 5.6 decreases with increasing temperature. This is in accordance with the results mentioned in the literature on others type of molecules [36]. All important information about the monolayers under investigation is summarized in Table 1.

Our investigation on hydroxamic acid monolayers was not confined to their non-dissociated state but at increased pH values on the dissociated form, too. The monolayer pressure-area isotherms of palmitoyl and stearyl hydroxamic acids on pure water sub-phase at different pH values can be correlated with the length of the carbon chain. As expected, under identical conditions the molecule with longer carbon chain gives a more rigid film than the shorter one. The stability of the C18HA monolayer increases with the increase of sub-phase pH from acidic to near neutral values up to about the pK value. At pH 5.6, a stable, compact film is obtained.

This behavior is supported by the surface demand of the C18HA molecules at different pH values. The pH dependence of the molecular area has shown a minimum at about 5.5. At extreme pH values, i.e., at acidic and espe-

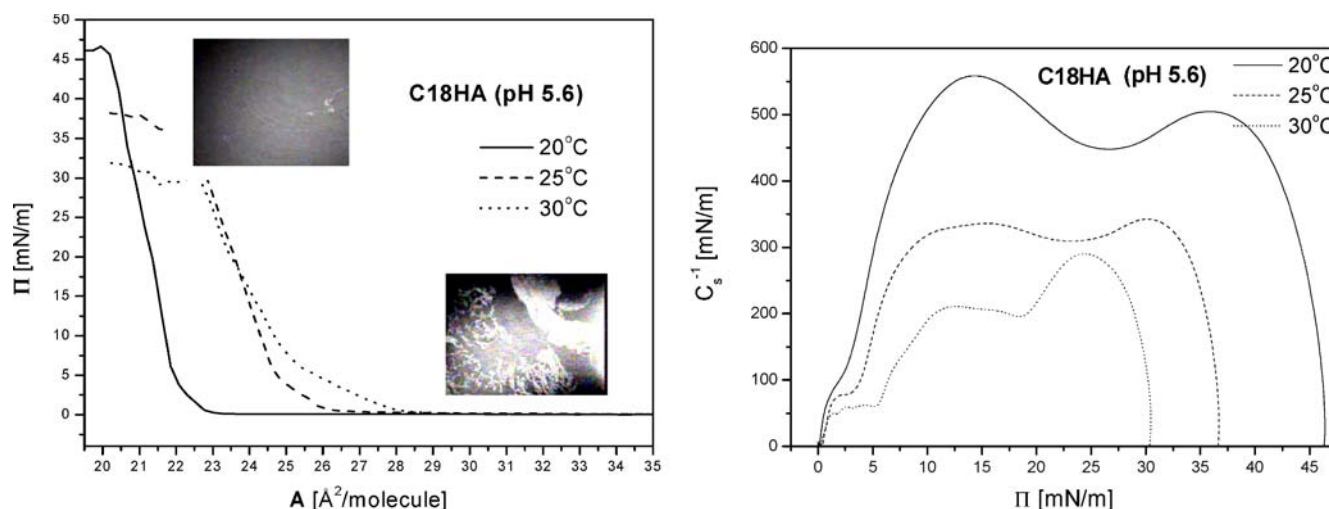


Fig. 1 Temperature dependent isotherms and compression modulus of the stearyl hydroxamic acid; BAM images taken at the “gas” phase as well as after collapse are inserted [30]

Table 1 Characteristic parameters of three amphiphiles

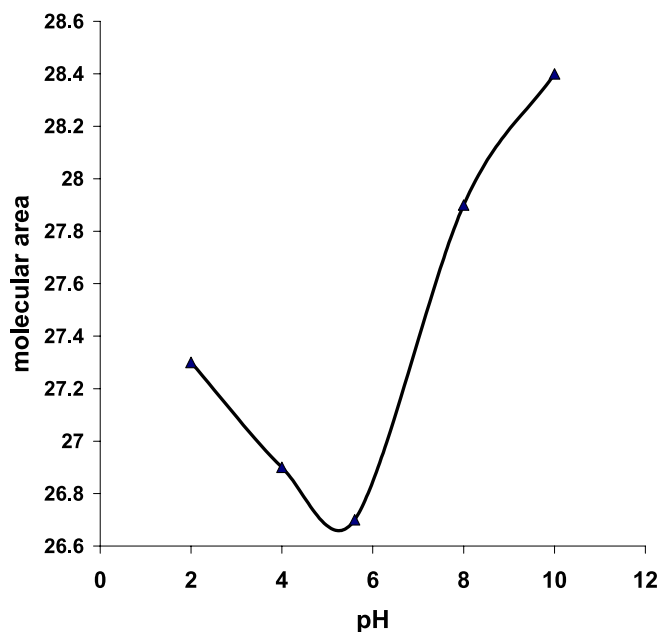
pH	Collapse pressure [mN/m]		
	C16N monolayer	C18N monolayer	C18P monolayer
2.0	35	35	31
4.0	29	33	27
5.6	28	33	29
8.0	27	33	31
10.0	26	34	–
<i>T</i> [°C]			
20	38	46	34
25	34	37	30
30	27	31	24
Molecular area [Å ² /molecule]	27	21	31

cially at alkali pH values these molecules occupy larger surface area, which may be due to the structure of the head group. Alkyl hydroxamic acid monolayers can dissociate at higher pH. The *pK* measured in solution is shifted in some cases to higher values on the water sub-phase [37].

As these hydroxamic compounds are weak acids, when the sub-phase is acidified to pH 2, their ionization is completely suppressed and they behave like neutral molecules. At this low pH (protonated structure, non-dissociated neutral molecules) the C(O)NHOH groups are switched by intermolecular hydrogen bonding, which gives 2D net of molecules. At a little higher pH value hydrogen ions dissociate from the hydroxamic acid and hydroxamate ions are involved into the molecular film. With increasing pH in the sub-phase, the dissociation of the individual molecule as well as the ratio of deprotonated groups increases. The hydrogen bond between protonated (–OH) and deprotonated groups (negatively charged O[–]) is stronger, around pH = 6 the head groups of the molecules require smaller area on the sub-phase. Competition between the hydrogen bond and electrostatic repulsion can be observed. At pH around the *pK* value the molecular area has a minimum, which may be due to the shorter intermolecular distance between protonated and deprotonated oxygen atoms. At higher pH values repulsion between charged head groups predominates, and the electrostatic repulsion counteracts with the van der Waals forces between the long carbon chains; the consequence is that the molecules require more area. The pH-dependent molecular area curve is asymmetric (Fig. 2).

The transition pressure between liquid and solid phases varies with the pH values of the sub-phase. At increasing pH values the transition pressure decreases, but the collapse pressure (when multi-layers are formed) is not significantly affected by it (Table 1).

In the first theoretical description of the Π/A isotherms given by De Boer [38] the van der Waals equation for non-

**Fig. 2** pH-dependent molecular areas in case of stearoyl hydroxamic acid

ideal two-dimensional gases is the follow

$$\Pi = RT/(A - \omega) - a/A^2, \quad (1)$$

(where *R*: gas constant, *T*: temperature, ω : the area per one molecule of the amphiphile in the extremely compressed monolayer, *A*: area available for molecules during two-dimensional condensation, *a* = molecular constant).

This predicts the existence of metastable state for the high values of the molecular constant *a* which is valid when the area available for molecules decreases but the surface pressure remains unchanged. When the surface pressure increases, the equation [39] is valid, when $A \geq A(c)$

$$\Pi = RT/(A - \omega) - B, \quad (2)$$

(*B*: intermolecular constant)

A(*c*) is the area available for the molecules at liquid-expanded/liquid-condensed state.

The pH- and temperature-dependent surface pressure/molecular experimental isotherms were used for the quantitative determination of intermolecular constants. The intermolecular constants calculated from Eq. 2 are summarized in Tables 2 and 3.

Not only the van der Waals interaction and hydrogen bond formation but electrostatic interactions also play important role in monolayer formation. According to the calculated intermolecular constants the van der Waals force increases with increasing alkyl chain. Table 3 summarizes the effect of pH on the intermolecular constants. At low pH a weaker hydrogen bond, at higher pH values the elec-

Table 2 Temperature-dependent intermolecular constants

	20 °C	<i>B</i> [mN/m] 25 °C	30 °C
	C16N	-0.0129	-0.0607
C18N	-0.0291	-0.1393	-0.1747

Table 3 The pH-dependent intermolecular constants

	<i>B</i> [mN/m]			
	pH = 2	pH = 4	pH = 5.6	pH = 8
C16N	-0.6771	-0.1639	-0.0607	-0.7766
C18N	-0.6833	-0.2933	-0.1393	-0.6084

trostatic repulsion modifies the van der Waals attraction. At pH 2 a lateral hydrogen bond network links the internal groups in the monolayer. At near neutral pH values stronger mutual forces lead to stable films. At alkaline pH range, because of strong electrostatic repulsion, the nanolayer structure shows less ordering, the aggregates are in small lace-like domains.

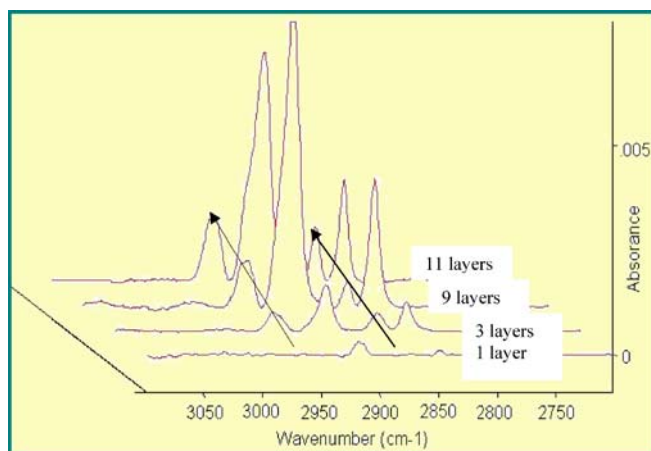
Characterization of the Nanolayers

Significant increase in contact angles has proven the successful layer deposition (Table 4). According to the literature [40], when the contact angle value of a nanolayer coated surface is less than 110°, the film on the solid is partly disordered or there are defect places in it. In our cases these values significantly exceed the 110° that prove the presence of films on metals with hydrophobic character and the existence of tightly packed methyl groups.

Infra red spectroscopic techniques are accepted methods for studying nanolayers as they provide information on the binding mode and on the molecular conformation and orientation. The time-dependent measurement of infra red reflectivity can also be used to monitor the adsorption. Our measurements were completed by IRRAS and SFG

Table 4 Contact angles measured in water on copper and iron surface with and without nanolayers

Surface	Control	Stearoyl hydroxamic acid LB monolayer	Octadecanoyl phosphonic acid LB monolayer
	Θ dyn adv./retr.	Θ dyn adv./retr.	Θ dyn adv./retr.
Copper	78°/31°	128°/95°	124°/88°
Iron	68°/32°	123°/72°	126°/95°

**Fig. 3** IRRAS spectra of LB nanolayers of stearyl hydroxamic acid deposited onto copper

measurement. The first technique has proven a successful layer-by-layer deposition (Fig. 3). On copper or iron substrates in case of monolayer a perpendicular molecular arrangement and a tilted one in multi-layers (up to 9) was observed. The average tilt angle is around 23°. Linear relationship was observed between the number of layers and the asymmetric and symmetric CH₃ stretching band intensity (with $R^2 = 0.9992$). The other type of well-ordered structure is involved into SAM layers. The chain-length and deposition time-dependent increase in intensity got by these techniques has helped to prepare compact SAM layers (Figs. 4 and 5). These methods are very complementary because not only the adsorption and the layer-by-layer deposition are detected but also the completeness of the SAM process is demonstrated. The SFG reflectivity gives information about secondary processes like increasing ordering in the nanolayers at the surface [41, 42]. In the nanolayers of hydroxamic acids (like in the case of fatty acids [43, 44]) the alkyl chains are in all-trans conformation with their long axis normal to the substrate.

Electrochemical Measurements

The anticorrosion efficiency of the nanolayers measured by electrochemical polarisation is demonstrated in Table 5.

The efficiency data show that the hydroxamic acid nanolayers both in LB and SAM films decrease the corrosion processes and their influence slightly depends on the length of carbon chain of the amphiphiles.

Results of other electrochemical technique (EIS; Fig. 6) support the efficiency data got by polarization measurement. The polarization resistance (R_p) data (which are the measure of the nanolayer resistance in the corrosion process) increase significantly with increasing layer formation time. These films form insulating films between the aqueous aggressive environment and the metal surface

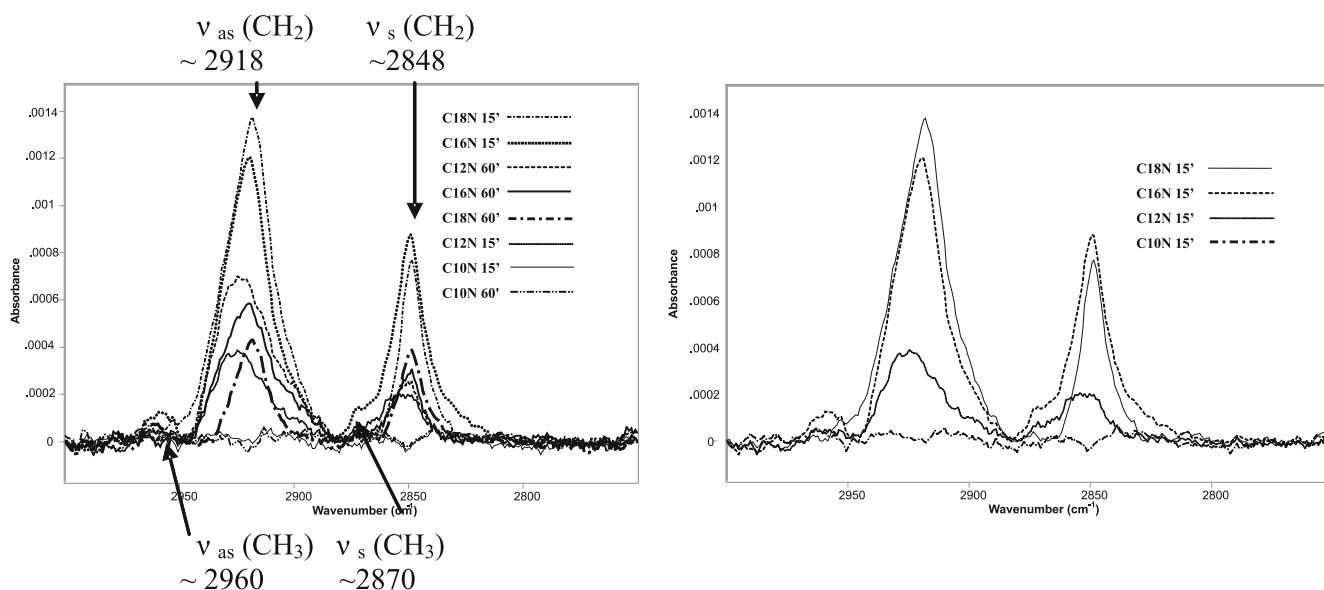


Fig. 4 SAM layers on copper surface; chain-length and time-dependent IRRAS spectra (0° polarization)

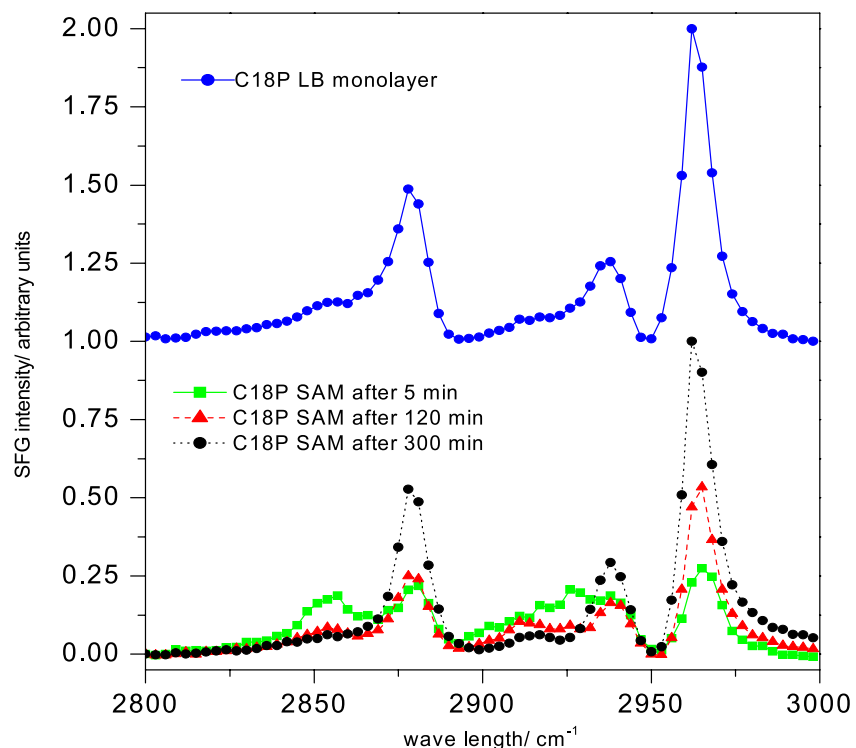


Fig. 5 SFG spectra of the octadecanoyl phosphonic acid in LB and time-dependent SAM layer deposited onto iron surface

and block the active places. Higher R_p values mean less porosity of the layer.

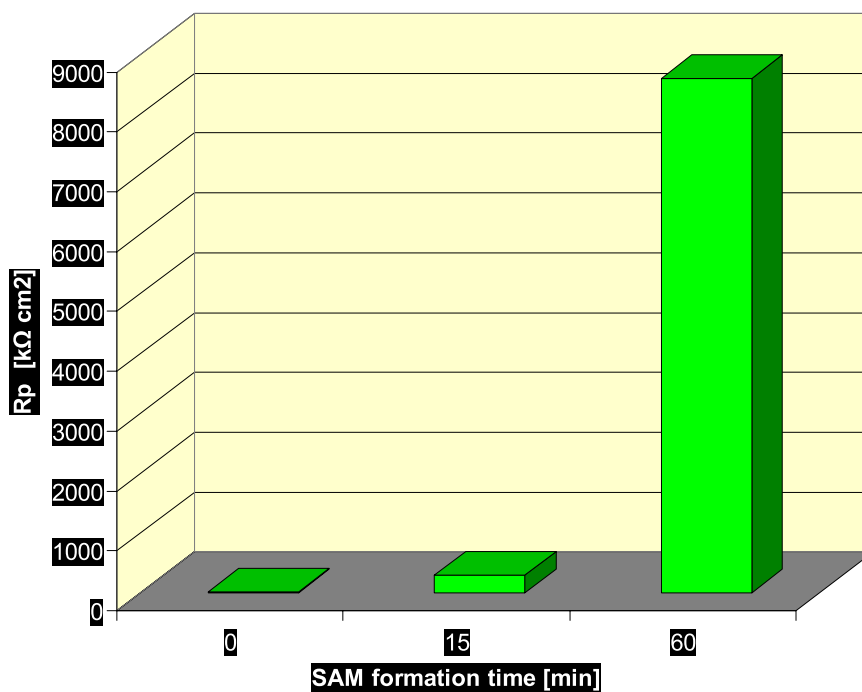
Control of Microbial Adhesion by Nanolayers

Desulfovibrio desulfuricans can much less adhere to nanocoated metal surfaces than to pure copper or iron

coupons (Fig. 7). Similar experimental results were observed on pyrite in the presence of *Acidithiobacillus ferrooxidans* and *Leptospirillum ferrooxidans* (Fig. 8; these microorganisms are responsible for bioleaching processes). The example of experiments carried out by pyrite coupons shows the effectiveness of multilayers in comparison with a monomolecular film. On copper and

Table 5 Results of anticorrosion experiments got in the presence of LB monomolecular films and SAM layers developed from hydroxamic acids, deposited onto copper electrodes (0.1 M Na₂SO₄, pH = 3; 23 °C; η = efficiency)

	E_{corr} [mV]	j_{corr} [$\mu\text{A cm}^{-2}$]	η [%]
Copper	-26	0.91	–
Cu + LB:palmitoyl hydroxamic acid	-29	0.35	62
Cu + LB:stearoyl hydroxamic acid	-31	0.25	73
Cu + SAM:decanoyl hydroxamic acid	-36	0.13	76
Cu + SAM:lauroyl hydroxamic acid	-38	0.17	81
Cu + SAM:palmitoyl hydroxamic acid	-39	0.16	82
Cu + SAM:stearoyl hydroxamic acid	-40	0.14	85



Measuring time [h] →	Rp [kΩcm ²]	
	1	20
SAM formation time [min]		
5	5	15
15	106	305
60	2564	8596

Fig. 6 Results of electrochemical impedance spectroscopic measurements with copper electrodes with and without SAM layers developed from decanoyl hydroxamic acid

iron coupons with and without nanocoatings after dipping into cooling water (Table 6), the number of the orange colored (dead) cells and green colored (vial) cells show how effectively the nanolayer could repel the microorganisms from the surface. The increase in SAM formation time and LB monomolecular layer number enhance the layer quality (ordering, compactness, porosity),

a more hydrophobic film can better inhibit the adhesion of microorganisms.

We tried to find a quantitative correlation between the surface properties and the number of adsorbed microorganisms. Table 6 summarizes the metal surface energies got from the contact angle values and the number of the microorganisms irreversible adsorbed onto the solids (with

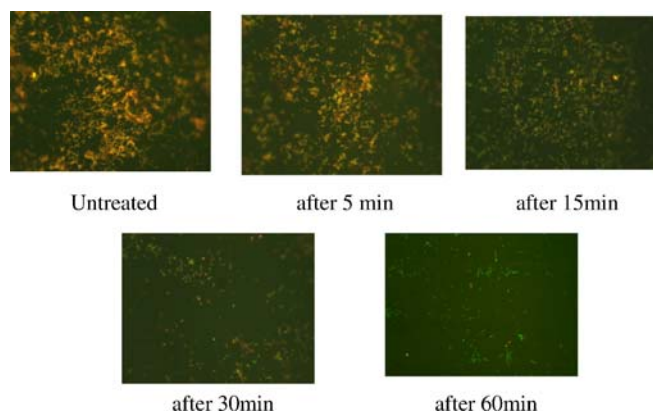


Fig. 7 Adhesion of *Desulfovibrio des.* on copper surface covered by SAM layer; influence of SAM layer formation time; the amphiphile is lauroyl hydroxamic acid

and without nanocoatings). The number of microorganisms of cooling water adhered to pure metal surfaces are larger with order of magnitudes than those measured on nanocoated surfaces. The only exception is the iron coated by C18P monolayer, which effectively inhibit the corrosion processes, but the adsorption of microorganisms is little decreased. From the measured contact angle values the surface energies were derived. It is well known that the surface energy of pure metals is high. Hydrophobic nanocoatings decrease this value. According to our experimental results the corrosion relevant microbes, which are covered by ionic biocoating, dislike the hydrophobic surface. Increase in surface energy results in decreased microbial number on the surface.

Conclusion

This paper has presented results on amphiphilic molecules in LB and SAM layers. The change in the pH and

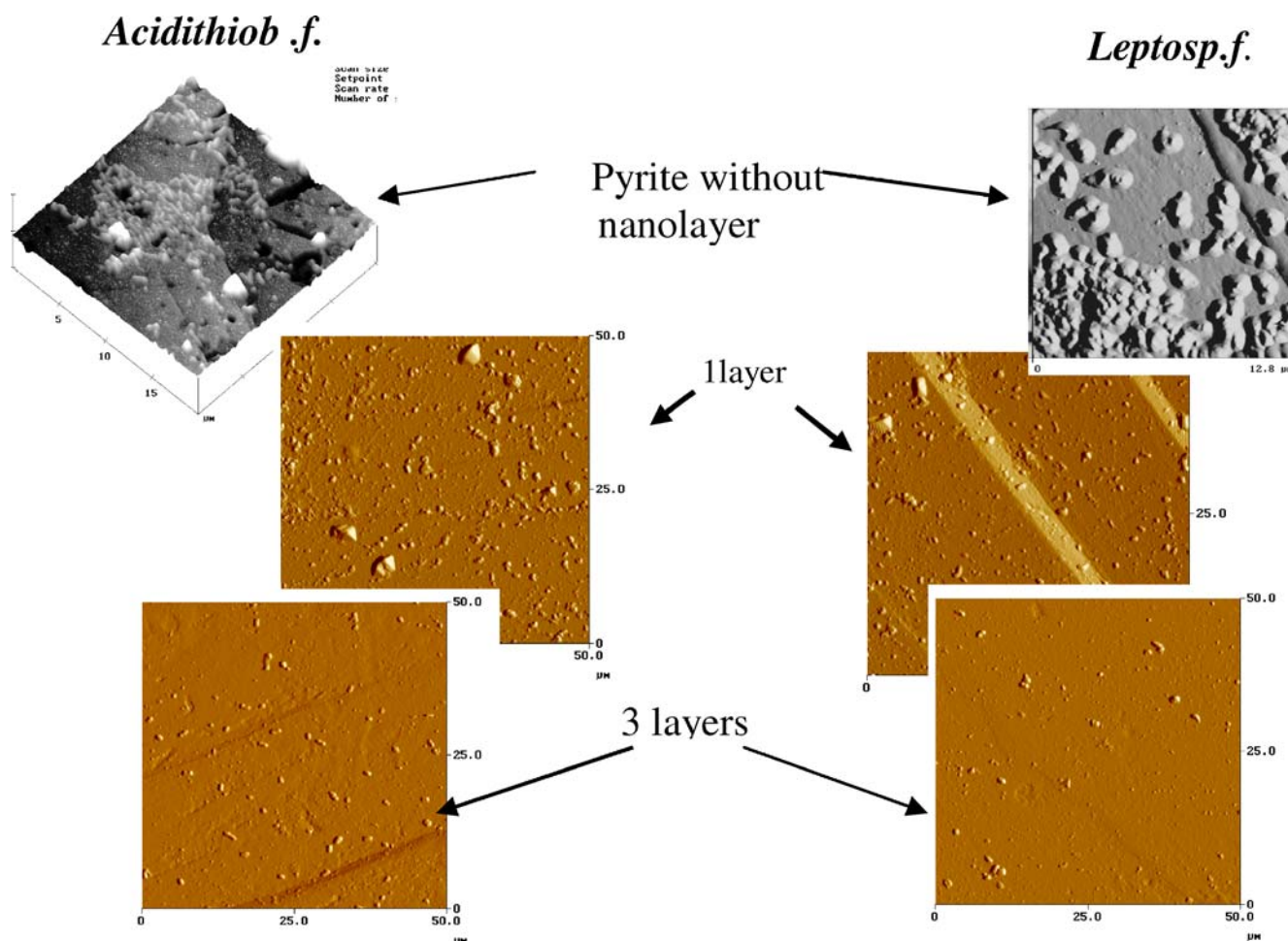


Fig. 8 Pyrite surfaces after immersion into media inoculated with *Acidithiobacillus ferrooxidans* and *Leptospirillum ferrooxidans*; influence of nanolayers onto the microbial adhesion

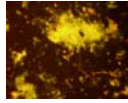
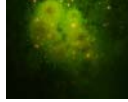

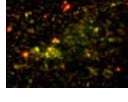

temperature values was reflected in isotherms of Langmuir monomolecular layer which allowed us to calculate characteristic parameters (molecular area, intermolecular constants etc.) of the hydroxamic and phosphonic acid amphiphiles. Contact angles, SFG and IRRAS techniques have rendered possible to characterize LB layers, to ascertain the most proper SAM layer formation time. By electrochemical measurements the anticorrosion effectiveness of these nanolayers has been proven. Positive correlation was found between the efficacy of nanofilms and

1. the molecular layer number in LB films;
2. the SAM layer developing time;
3. the carbon chain length in the amphiphiles.

These nanolayers could control not only the corrosion processes but the microbial adhesion too, that was ascertained by the correlation between the surface energy and the number of adhered microorganisms.

Acknowledgement This work was supported by Marie Curie Research Training Network (CHEXTAN). The authors convey their sincere thanks to Katalin Tímár for the synthetic work.

Table 6 Correlation between the surface energy and the microbial invasion on different, coated and uncoated surfaces (iron, copper, nanolayers, coupons in cooling water with for 5 days)

Metal	Surface energy [erg cm ⁻²]	Microorganisms in biofilm [cell cm ⁻²]	
Fe	62.99	5.2 × 10 ⁵	
Fe + LB:stearoyl hydroxamic acid	25.06	3.6 × 10 ³	
Fe + LB:octadecanoyl phosphonic acid	42.39	1.6 × 10 ⁵	
Cu	56.67	1.2 × 10 ⁵	
Cu + LB:stearoyl hydroxamic acid	25.66	6.8 × 10 ²	

References

1. Gaines GL (1966) Insoluble Nanolayers at liquid/gas interfaces. Interscience, New York
2. Petty MC (1996) Langmuir–Blodgett films. An Introduction. Cambridge Univ Press, Cambridge
3. Roberts GG (1990) Langmuir–Blodgett Films. Plenum Press, New York
4. Ulman A (1991) An Introduction to Ultrathin Organic Films, from LB to Self Assembly. Academic Press, San Diego
5. Schwartz DK (1997) Surf Sci Rep 27:241
6. Roberts GG (1985) Adv Phys 34:475
7. Swalen JD, Allara DL, Andrade JD et al. (1987) Langmuir 3:932
8. Petersen IR (1994) In: Mahler G, May V, Schreiber M (eds) The Molecular Electronic Handbook. Marcel Decker, New York
9. Mohai M, Kiss É, Tóth A, Szalma J, Bertóti I (2002) Surf Interf Anal 34:772
10. Allara DL, Nuzzo RG (1985) Langmuir 1:45 and 52
11. Slotter NE, Porter MD, Bright TB, Allara DL (1986) Chem Phys Lett 132:93
12. Thoughton EB (1988) Langmuir 4:365
13. Laibinis PE (1991) J Am Chem Soc 113:7152
14. Laibinis PE, Whitesides AM (1992) J Am Chem Soc 114:9022
15. Jennings GK, Munkro JM, Yong TH, Laibinis PE (1998) Langmuir 14:6130
16. Van Alsten JG (1999) Langmuir 15:7605
17. Lossen H (1869) Justus Liebigs Ann Chem 150:134
18. Miller MJ (1989) Chem Rev 89:1563
19. Nagarajan K, Rajappa S, Rajagopalam P et al. (1991) Indian J Chem B 30:222
20. Nakamura S, Inouye Y (1989) Kagaku Zokan (Kyoto) 116
21. Schmetzer J, Stetter J, Hammann I, Homeyer B (1982) Eur Pat 50, p 283
22. Farkas E, Megyeri K, Somsák L, Kovács LJ (1998) Inorg Biochem 70:41
23. Farkas E, Enyedi ÉA, Csóka H (1999) Polyhedron 18:23910
24. Farkas E, Enyedi ÉA, Csóka H (2000) J Inorg Biochem 79:205
25. Farkas É, Enyedi A, Zékány L, Deák G (2001) J Inorg Biochem 83:107
26. Shaban A, Kálmán E, Telegdi J (1998) J Electrochim Acta 43:159
27. Alaghta A, Felhősi I, Telegdi J, Bertóti I, Kálmán E (2007) Corr Sci 49:2754
28. Folkers JP, Gorman CB, Laibinis PE et al. (1995) Langmuir 11:813
29. Deng H, Nanjo H, Qian P et al. (2008) Electrochim Acta 53:2972
30. Telegdi J, Rigó T, Kálmán E (2005) J Electroanal Chem 582:191
31. Telegdi J, Rigó T, Kálmán E (2004) Corr Eng Sci Technol 39:65
32. Telegdi J, Rigó T, Beczner J, Kálmán E (2005) Surf Eng 21:1
33. Hauser CR, Renfrow WB (1971) Org Synth Collect 2.67
34. Baret F, Hasmonay H, Firpo J et al. (1982) Chem Phys Lipids 30:177
35. Seoane R, Miñones J, Conde O et al. (2000) J Phys Chem B 104:7735
36. Kang YS, Lee DK, Kim YS (2001) Synth Met 117:165
37. Betts JJ, Pethica BA (1956) Trans Faraday Soc 52:1581

-
38. De Boer JH (1945) *The Dynamical Characters of Adsorption*. Oxford Univ Press, London
 39. Jasper JJ (1972) *J Phys Chem Ref Data* 1:841
 40. Engelking J, Wittemann M, Rehahn M, Menzel H (2000) *Langmuir* 16:3407
 41. Schnitter M, Engelking J, Heise A, Miller RD, Menzel H (2000) *Macromol Chem Phys* 201:1504
 42. Umemura J, Takeda S, Hasegawa T, Takenaka T (1993) *J Mol Struct* 297:57
 43. Kimura F, Umemura J, Takenaka T (1986) *Langmuir* 2:96
 44. Holland RF, Nielsen JR (1962) *J Mol Spectrosc* 9:436